Calculation of ironless Permanent Magnet couplings using semi numerical magnetic pole theory method

Jean-Frederic Charpentier, Guy Lemarquand

▶ To cite this version:

HAL Id: hal-01208077

https://hal.archives-ouvertes.fr/hal-01208077

Submitted on 1 Oct 2015

Calculation of ironless Permanent Magnet couplings using semi numerical magnetic pole theory method

Abstract

This paper deals with a way of computation of the mechanical behavior of Permanent Magnet synchronous couplings . This method is based on the calculation of the forces between the magnets of the device. The formulation of these forces is based on magnetic pole theory. The computation is done using a semi-numerical integration method. This method has been validated in test cases and appears to be very advantageous in terms of calculation time and precision. So this solution appears to be a good way to study and design this kind of devices.

keywords : **Permanent Magnet, Modelling, Force, Torque, Coupling**

Introduction

Synchronous Permanent Magnet couplings are used in many applications to transmit a torque from one rotor to another without any contact and without any friction

(Elies,1998),(Giannini,1982). These devices are very useful in sealed equipment to avoid contamination between two different media. They are used when a high efficiency is wanted because they allow to eliminate the mechanical losses. They can also be used in many secure equipment to avoid a failure due to a torque overload.

The main design specifications for this kind of structure are its pull-out torque which is the maximal torque which can be transmitted by the coupling and its mechanical behavior in terms of stability (forces and stiffnesses on the rotors) (Yonnet,1981).

This paper deals with a way of study of ironless couplings. These ironless couplings have a very small inertia and can be advantageous in many applications (Charpentier,1999).

A classical way to study this kind of devices is the 2D or 3D Finite Element method which allows to compute the torque and forces exerted on the two rotors (Feirera,1989)(Wu,1997). However this solution is very heavy in terms of calculation time. The calculation precision with FE method is very sensible to mesh density and to the formulation. So this type of calculation can be not advantageous in terms of precision to calculate the characteristics of the couplings.

So it can be difficult to do a systematic study of these devices using FE analysis.

Some authors have developed analytical and semi-analytical models to study the synchronous PM couplings (Overshott,1989),(Furlani,1995),(Furlani,1996).

This paper deals with an interesting way of calculation of the characteristics of the

ironless PM couplings. This method is very general and is based on the calculation of the forces between the magnets of the structure. This calculation is done using a semi-numerical method based on magnetic pole theory.

The obtained results are then compared with a classical finite element method and appears to be very efficient to study this type of devices in terms of precision and calculation time.

Presentation of the devices

The synchronous Permanent Magnet ironless couplings consist of two rotors. The first one is the leading rotor and the second one is the led rotor. This kind of structure allows to transmit a torque from one rotor to the other without any contact.

The two rotors are build with parallelepipedical Permanent Magnets stuck in ironless cores. Two configurations are the more often encountered in industrial applications. The first one is a cylindrical air gap coupling where radially oriented magnets are stuck in an inner and outer rotor and where the air gap is cylindrical. The second one is a plane air gap coupling where the two rotors are separated by a plane air-gap and the magnets are oriented axially.

Figure 1-a presents an example of a cylindrical air gap coupling with 10 poles. This coupling is shown in the zero torque stable position.

In Figure 1-b an example of a 6 poles plane air gap axial coupling is presented.

3

This coupling is also shown in its zero torque stable position.

Cylindrical air gap coupling (10 poles)
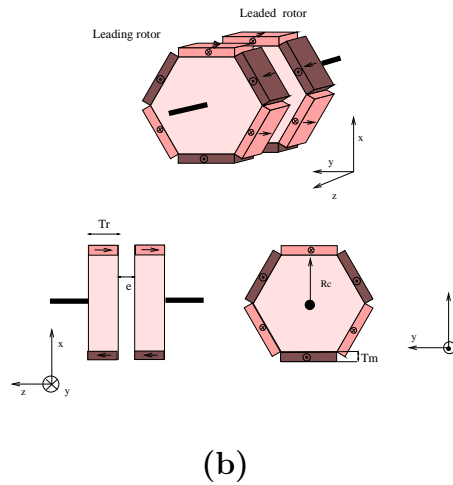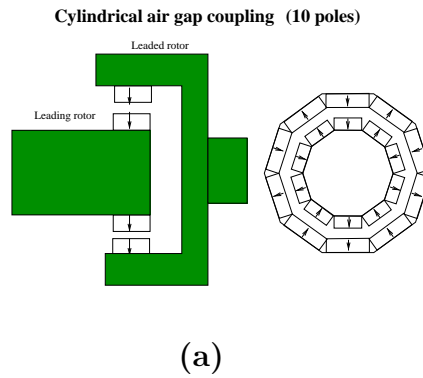

(a)

(b)

Figure 1: cylindrical coupling (a) and plane air gap coupling (b)

These two kinds of structure are the most useful in industrial applications. However non classical structures may be also studied and used (Lemarquand,1999) (Charpentier,1999)

Magneto-mechanical characteristics Calculation Method

These devices are characterized by the torque exerted by one rotor on the other. This torque is a function of the relative angular position of the two rotors. So each mechanical load torque corresponds to an angular shift between the two rotors. The maximal value of this torque versus the angular shift between the rotors is the maximum value of the torque which can be transmitted by the coupling. This value is called pull-out torque and is the main specification for the design of such a coupling.

Another very important magneto-mechanical characteristic of the PM couplings is the mechanical stability of the coupling. This stability is characterized by the forces and the stiffnesses exerted by one rotor to the other.

The computation of the torque and the mechanical behavior of ironless PM couplings can be done by the calculation of the magnetic forces exerted on each magnet of rotor 2 (led rotor) by each magnet of the rotor one (leading rotor).

The torque exerted on rotor 2 by rotor 1 can be easily calculated by the knowledge of the tangential components of the forces exerted on one magnet of the second rotor by all the magnets of the first rotor. The torque can be expressed as :

$$T = 2p(\sum_{i \in \text{ rotor } 1} F_t(i).r_2) \tag{1}$$

where $F_t(i)$ is the tangential component of the force exerted by the magnet i of the first rotor on one magnet of the second rotor , r_2 is the average radius of this magnet

5

and p is the number of pole pairs.

By using this method the torque can be calculated for any angular position of the two rotors.

The global force exerted by the first rotor on the second rotor can be calculated as the sum of the forces $\mathbf{F(i,j)}$ exerted by the magnets i of the first rotor on the magnets j of the second rotor.

$$\mathbf{F} = (\sum_{i \in \text{ rotor } 1} (\sum_{j \in \text{ rotor } 2} \mathbf{F(i,j)})) \tag{2}$$

The stability and the behaviour of the device in terms of vibration can be characterized by the stiffnesses defined by the following relations :

$$K_x = -\frac{\partial F_x}{\partial x} \tag{3}$$

$$K_y = -\frac{\partial F_y}{\partial y} \tag{4}$$

$$K_z = -\frac{\partial F_z}{\partial z} \tag{5}$$

The stiffness of the coupling in the x axis (resp. y and z) can be calculated for any angular shift θ between the two rotors, considering a very small displacement, dx, of the second rotor along the x (respectively y or z) axis. The x (resp. y or z) component of the force exerted on the second rotor must be calculated for the two positions of the second rotor (O position and dx position). Then the stiffness K_x (resp K_y and K_z) of the coupling in the x axis (resp. y and z) can be estimated as :

$$K_x(\theta) = -\frac{F_x(\theta, dx) - F_x(\theta, 0)}{dx} \tag{6}$$

6

Where $\mathbf{K_x}(\theta)$ is the stiffness in the x axis, $F_x(\theta, dx)$ is the x component of the force exerted on rotor two when this rotor is shifted in the displacement dx. $F_x(\theta, 0)$ is the x component of the force exerted on rotor two when this rotor is not shifted.

Forces between magnets

We have seen that the calculation of the magneto-mechanical characteristics of the coupling can be done by the computation of the forces exerted between the magnets of the coupling. We present here a very general solution which allows the calculation of the force exerted by one magnet to another. This way of calculation is based on the magnetic pole theory method and a semi-numerical integration method.

Field created by a magnet

According to magnetic pole theory a parallelepipedical magnet dimension (a,b,c)can be considered like two charged planes. One of this plane, S_{1+}, is charged with positive magnetic charges and the other, S_{1-}, with negative magnetic charges as shown in Fig. 2. The charge density in each plane is equal to $\vec{J}.\vec{n}$, where $\vec{J}$ is the material magnetization and $\vec{n}$ is the normal vector on the surfaces. So the the magnetic induction created by a magnet in a P point (x,y,z) in free space can be seen as the
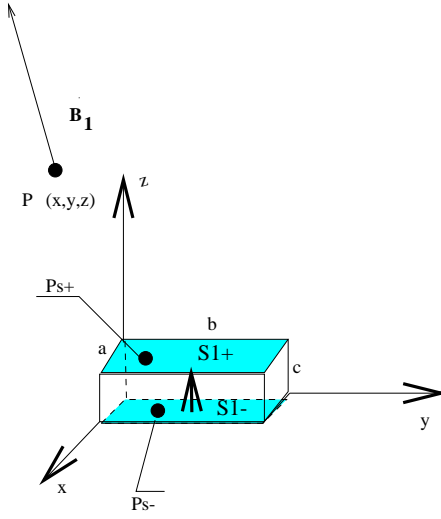
7

Figure 2: Field created by a magnet

superposition of the two fields created by each of the two charged planes.

$$\overrightarrow{B_1} = \int\int_{S_{1+}} \frac{J}{4\pi} \frac{\overrightarrow{P_S^+ P}}{{P_S^+ P}^3} dS_{1+} - \int\int_{S_{1-}} \frac{J}{4\pi} \frac{\overrightarrow{P_S^- P}}{{P_S^- P}^3} dS_{1-} \tag{7}$$

This formula can be analytically expressed in the 3 axis (Bancel,1998) (Akoun,1984).

$$
\begin{aligned}
B_{1x}(x,y,z,a,b,c,J_0) &= \frac{J}{4\pi} \ln\left[\frac{N_x(x,y,z,a,b,c)N_x(x,y,z,0,0,c)N_x(x,y,z,a,0,0)N_x(x,y,z,0,b,0)}{N_x(x,y,z,a,0,c)N_x(x,y,z,0,b,c)N_x(x,y,z,a,b,0)N_x(x,y,z,0,0,0)}\right] \\[2mm]
B_{1y}(x,y,z,a,b,c,J_0) &= \frac{J}{4\pi} \ln\left[\frac{N_y(x,y,z,a,b,c)N_y(x,y,z,0,0,c)N_y(x,y,z,a,0,0)N_y(x,y,z,0,b,0)}{N_y(x,y,z,a,0,c)N_y(x,y,z,0,b,c)N_y(x,y,z,a,b,0)N_y(x,y,z,0,0,0)}\right] \\[2mm]
B_{1z}(x,y,z,a,b,c,J_0) &= -\frac{J}{4\pi}
\begin{bmatrix}
N_z(x,y,z,a,b,c) - N_z(x,y,z,a,b,0) \\[2mm]
-N_z(x,y,z,a,0,c) + N_z(x,y,z,a,0,0) \\[2mm]
-N_z(x,y,z,0,b,c) + N_z(x,y,z,0,b,0) \\[2mm]
+N_z(x,y,z,0,0,c) - N_z(x,y,z,0,0,0)
\end{bmatrix}
\end{aligned}
\tag{8}
$$

8

where

$$N_x(x, y, z, a, b, c) \quad = \quad b - y + \sqrt{(x-a)^2 + (y-b)^2 + (z-c)^2}$$

$$N_y(x, y, z, a, b, c) \quad = \quad a - x + \sqrt{(x-a)^2 + (y-b)^2 + (z-c)^2}$$

$$N_z(x, y, z, a, b, c) \quad = \quad \arctan \frac{(a-x)(b-y)}{(c-z)\sqrt{(x-a)^2 + (y-b)^2 + (z-c)^2}}$$

Forces between two magnets

The forces between two different magnets in any position can be deduced from the field produced by the first magnet on the charged planes of the second magnet, S_{2-} and S_{2+}, as shown in Fig. 3.
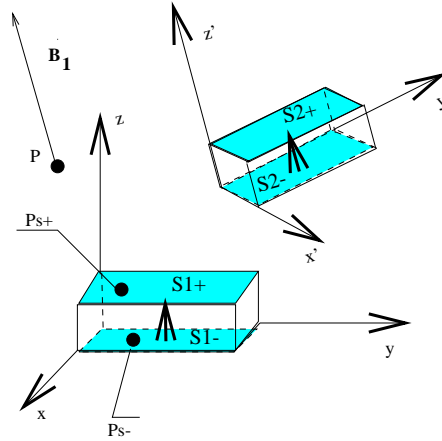

Figure 3: Force between two magnets

So the forces exerted by the first magnet on a second magnet can be expressed as :

$$\overrightarrow{F} = \iint_{S_{2+}} J\overrightarrow{H_1}dS_{2+} - \iint_{S_{2-}} J\overrightarrow{H_1}dS_{2-} \tag{9}$$

where dS_{2+} and dS_{2-} are equal to $dx'dy'$.

So this formula in free space gives :

$$\overrightarrow{F} = \iint_{S_{2+}} \frac{J}{\mu_0}\overrightarrow{B_1}dS_{2+} - \iint_{S_{2+}} \frac{J}{\mu_0}\overrightarrow{B}dS_{2+} \tag{10}$$

In the particular configuration shown in Fig. 4 , which is encountered in cylindrical air gap devices, two component of the force between two parallelepipedical magnets of the devices can be calculated in analytical way (Elies,1998). This solution allows
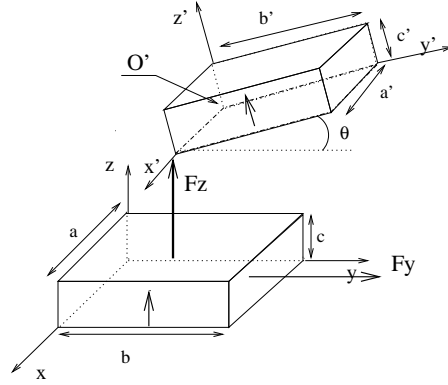

Figure 4: cylindrical air gap magnet configuration

to calculate the torque of such a device and the forces exerted by one rotor on the other in the radial direction. However the forces in the axial direction can not be calculated by this way. So this analytical way of calculation allows only the study of

10

radial air gap couplings in terms of torque (Charpentier,1999)(Elies,1998), but not in terms of mechanical stability.

In a general case and in the particular case of the plane air gap coupling configuration, an analytical solution of eq. 9 has not been found. However a solution of this equation can be computed using a numerical integration method like the Gauss and Labotto based integration method (Patterson,1968). This method allows to estimate numerically the double integral of eq. 9 with a very good precision. So the forces exerted between two parallelepipedical magnets in any relative position can be calculated with a good accuracy. So this semi-analytical solution allows the study of all the ironless couplings with parallelepipedical magnets in terms of torque and mechanical stability.

Illustration case

To illustrate the calculation of the forces exerted between two magnet using semi-numerical magnetic pole theory, we study here the tangential (f_t) , radial (f_r) and axial (f_a) components of the force exerted on one magnet (Magnet 1) by another magnet (Magnet 2). Magnet 2 is facing magnet 1, and rotate around an axis as shown in Fig. 5. The two magnets remain parallel. The magnetization of the two magnets is oriented along the rotation axis. This configuration corresponds to the position encountered in a classical plane air gap coupling. The calculation is done for

11

the following set of dimensions :

- the two magnets are cuboidal ($a = b = c = a' = b' = c' = 10mm$)

- the air-gap between the two magnets, e, is equal to $10mm$

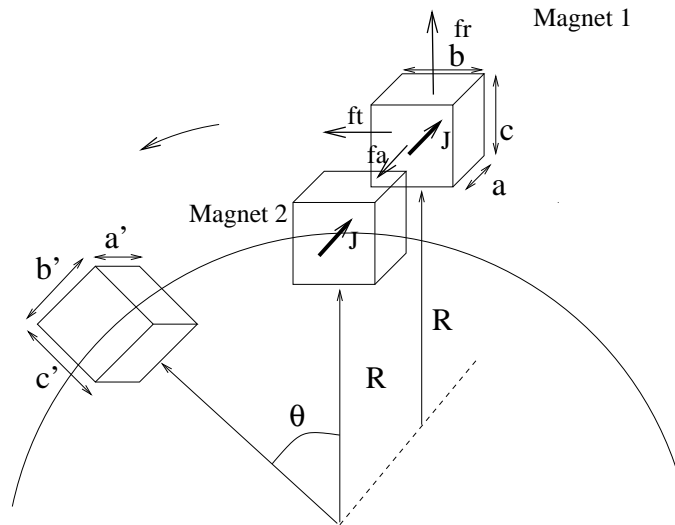- the magnet magnetization, J, is equal to $1T$

Figure 5: illustration case configuration

The computed forces are given in Fig. 6 as functions of the angular shift θ between the two magnets. We can notice that the 3 curves are symmetrical around the $\theta = 0$ position. This position corresponds to the stable configuration where the two magnets are facing each other. In this position the radial and tangential component of the force exerted on Magnet 1 are null and the axial component of the force reaches to
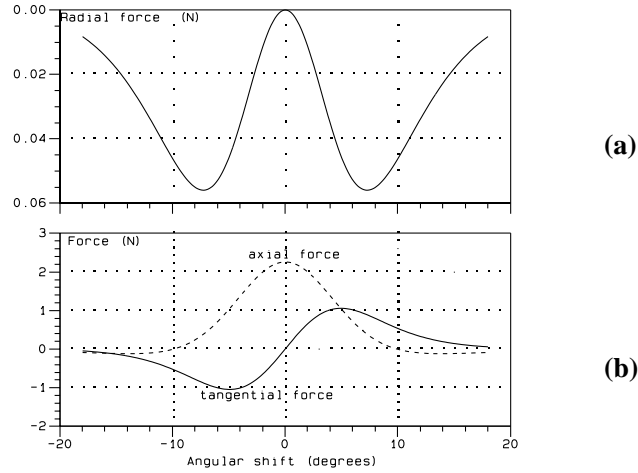
Figure 6: Radial forces (a), tangential and axial forces (b)

a maximum value. When the shift between the magnets increases, the tangential component of the force reaches to a maximum and then decreases. This maximal value corresponds to a compromise between the shift of the magnet in the tangential direction and the distance between the charged faces of the magnets. The radial component of the force remains very small in comparison with the axial and tangential components. That can be explained because, when the magnet are close, the shift of the two magnets in the axis direction remains very small. This example of illustration shows that the magnetic pole theory method can be a good tool for the 3D calculation of the forces exerted between two magnets.

13

Comparison with 3D Finite Element method in a test case

To validate and evaluate this method of calculation, we have compared this way of calculation with the classical 3D FE method in a test case. This test case is presented in Figure 7. It corresponds to the classical configuration encountered in plane air gap devices : two magnets, magnetized along the z axis, are facing each other (the charged faces are parallel). In this test case one of these magnets has rotated around one of its edge of 30 degrees. The magnet magnetization, J, is equal to $1T$.
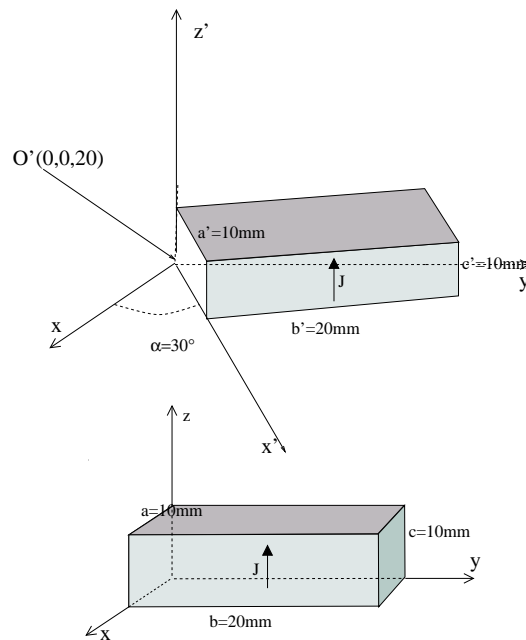

Figure 7: test case

The force components in the 3 axes (x,y and z) are computed using semi-numerical magnetic pole theory method and with 3D Finite Element method for different mesh

Mesh	Total Number of nodes	Force on magnet 1 (Fx,Fy,Fz) Newtons	Force on magnet 2 (Fx,Fy,Fz) Newtons
3D FE scalar potential formulation			
Mesh A	2060 nodes	-1.8, 0.6, 3.3	3.4, -3.0, -3.1
Mesh B	5048 nodes	-1.9, 0.2, 3.6	2.1, 0.1,- 2.9
Mesh C	14441 nodes	-2.2, 0.4, 3.8	2.5, 0.1, -3.3
Mesh D	54130 nodes	-2.6, 0.5, 3.8	2.1, -0.04 , -3.7
Mesh E	92255 nodes	-2.3, 0.002, 4.1	2.6, -0.04, -3.6
3D FE vector potential formulation			
Mesh D	54130 nodes	-2.5, 0.13, 4.0	2.4, -0.2, -4.4
Magnetic pole theory semi-numerical method			
		-2.5, 0.063, 4.15	2.5, -0.063, -4.15

Table I: Force results for 3D FE and semi-numerical methods

densities and different formulations : different mesh densities are used with a scalar potential formulation, and another calculation is done for the fourth one of these meshes, with a vector potential formulation. Used elements are first order tetrahedrons

In these calculations the force exerted on magnet 1 and the force exerted on magnet 2 are evaluated. Table I gives the obtained results for all these cases.

15

We can notice that in the FE cases the forces calculated on magnet 1 are not equal to the opposite of the forces exerted on magnet 2. This assumption shows that the precision of this method is not very convenient. However when the mesh density increases the differences between the forces exerted on magnet 1 and on magnet 2 decrease. That means that the calculation accuracy also increases. If we want to obtain a good precision, the mesh density must be very important and then the calculation time becomes prohibitive. We can also notice that the results obtained with a scalar potential formulation are quite different of the results obtained with a vector potential formulation for the same mesh. This means that, with a 3D FE method, the precision of calculation of the force between two magnets depends of the mesh density and of the formulation.

However when the mesh density is important the values of forces calculated with a 3D FE method are close of the results obtained with the magnetic pole theory semi-numerical method. We can notice too that the calculation of the force using the magnetic pole theory method is quasi immediate.

So the magnetic pole theory method appears to be validated and seems to be much more efficient than the classical FE method for this kind of problem in terms of precision and calculation time.

Various shapes of magnets

This general method of calculation can be applied to various shapes of magnet.

As an example an axially magnetized cylinder can be considered like two charged disks as shown in Fig 8. The charge density in each of these charged surfaces is equal to $\vec{J}.\vec{n}$ where $\vec{J}$ is the material magnetization and $\vec{n}$ is the normal vector of the surfaces.
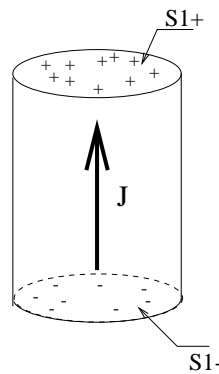

Figure 8: magnetized cylinder

So the field created by such a magnet in a P point can be evaluated integrating numerically the equation :

$$\overrightarrow{B_1} = \int\int_{S_{1+}} \frac{J}{4\pi} \frac{\overrightarrow{P_S^+ P}}{\overline{P_S^+ P}^3} dS_{1+} - \int\int_{S_{1-}} \frac{J}{4\pi} \frac{\overrightarrow{P_S^- P}}{\overline{P_S^- P}^3} dS_{1-} \tag{11}$$

where S_{1+}, S_{1-} are the charged disks at the extremities of the magnet. So the forces exerted by a cylindrical magnet axially magnetized on another magnet, can be evaluated by the way of numerical integration of the following equation :

17

$$\overrightarrow{F} = \iint_{S_{2+}} \frac{J}{\mu_0} \overrightarrow{B_1} dS_{2+} - \iint_{S_{2+}} \frac{J}{\mu_0} \overrightarrow{B} dS_{2+} \tag{12}$$

Where the second magnet is also represented as two charged surfaces S_{2+} and S_{2-}.

We can notice that another kind of magnets can be also considered using magnetic pole theory as two surfaces charged with magnetic charges : radially magnetized cylindrical tiles, triangular magnets as shown in Fig 9, and many other shapes of magnets.
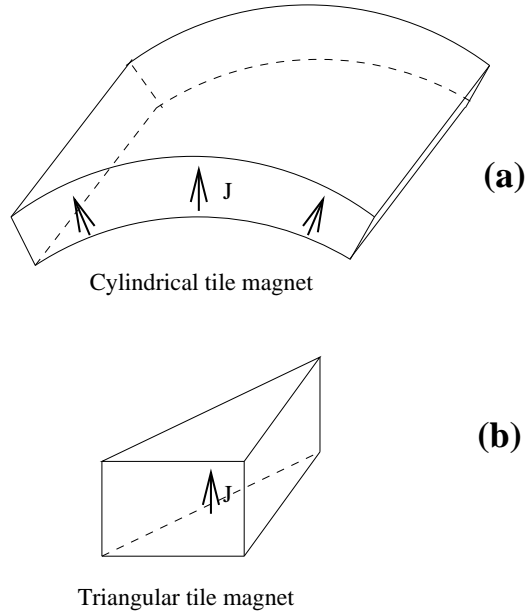

Figure 9: Other shapes of magnets : (a) cylindrical tile; (b) triangular tile

That means that the field and forces generated by this kind of magnets on other magnets can be also evaluated by this general semi-numerical method. So the per-

18

manent magnet magneto-mechanical devices where this kind of magnet are used can be studied with success by using this method.

Example of application : general study of plane air gap coupling

General considerations on torque

First we have calculated the torque exerted on one rotor by the other in a 24 poles plane air gap coupling as a function of the angular shift between the two rotors. The main dimensions of the studied coupling are presented in Table II. Figure 10 shows

Significance	Symbol in Fig. 1-b	Value
Core radius	Rc	90 mm
Magnet thickness	Tm	1O mm
Rotor thickness	Tr	10 mm
Air gap	e	2 mm
Magnet magnetization	J	1 T

Table II: Dimensions of the validation example

the evolution of the torque exerted on one rotor by the other versus the angular shift between the two rotors. The curve is of course periodical and the period corresponds to an angular shift of 2 θ_p, where θ_p is the angular value of a pole pitch. The maximum value of the torque when the angular shift varies is the pull-out torque of the device

19

(43 N.m). This value corresponds to the configuration where the two rotors are shifted by half a pole pitch.

The zero torque stable position (0 position) corresponds to the configuration where the north poles of rotor 1 are facing the south poles of rotor 2.

The calculation time necessary to do this computation (60 angular positions) is only around 30 seconds in a Pentium II 350 MHz under Linux O.S.
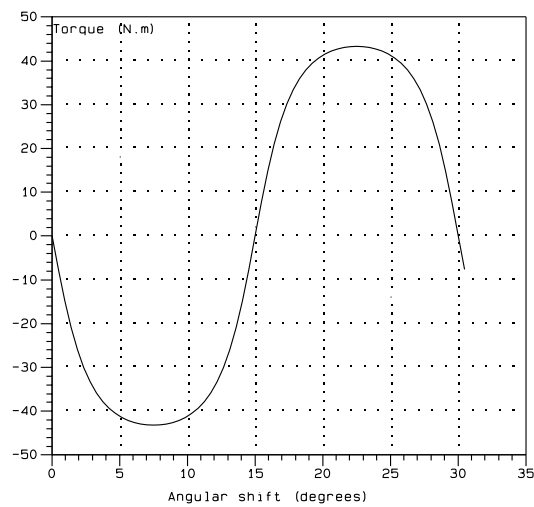

Figure 10: Torque exerted on one rotor versus angular shift

Influence of the number of pole pairs on the pull-out torque

In the second part of the study we want to show the influence of the number of pole pairs on the pull-out torque of a plane air gap couplings with axially magnetized

magnets. To study this influence we calculate the pull-out torque for the same characteristic dimensions than for the precedent example when the number of pole pairs varies. These dimensions are given in Table II. With this common set of dimensions the magnet volume remains approximatively constant for all the studied number of pole pairs. Figure 11 gives the evolution of the pull-out torque as a function of the number of pole pairs. We can notice that the curve presents a maximum for 27 pole pairs (This maximal value of the pull-out torque is equal to 63.25 N.m) . This optimal number of pole pairs corresponds to a quasi square section for the magnets. A similar result has been found for the cylindrical air gap ironless P.M. couplings (Elies,1998),(Charpentier,1999).
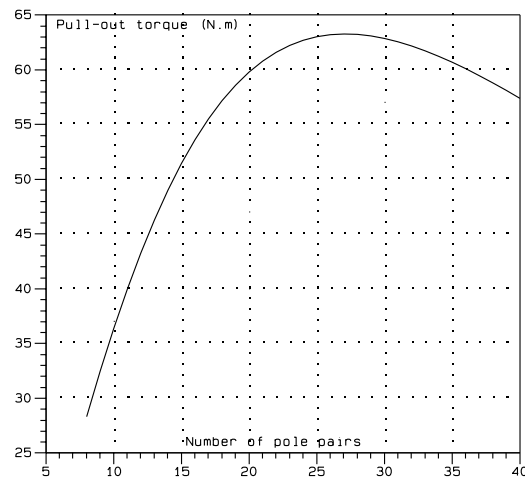

Figure 11: Pull-out torque versus number of pole pairs

21

General study of stability

For the same set of dimensions (Table II) and for the optimal number of pole pairs (27 pole pairs), we have studied the evolution of the forces and the stiffnesses of the coupling as a function of the angular shift between the rotors. Figure 12 shows the evolution of the torque and the axial force exerted on one of the rotors when the angular relative position between the rotors varies and when the rotors remain centered.
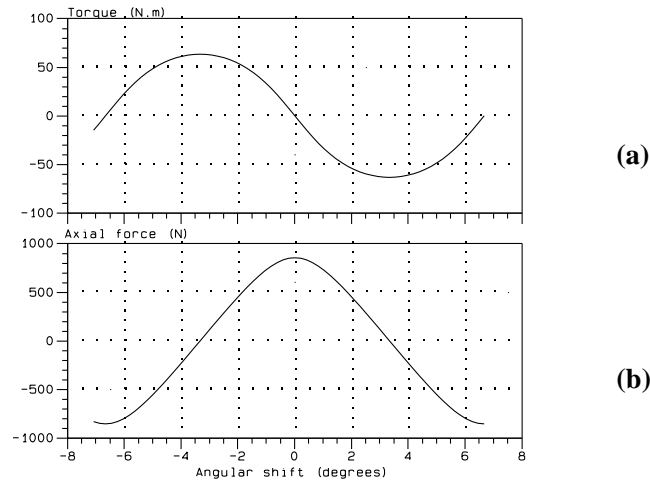

Figure 12: Torque (a) and axial force (b)

In this case, the force exerted on one rotor is axially oriented : the components of the forces which are perpendicular to the axis (fx,fy) are null for symmetry reasons. The axial force exerted on each of the rotors presents maximal values for the zero

torque positions where the magnets of the rotor 1 are facing the magnets of the rotor 2. In the operating conditions, the angular shift between the rotor is between $-\frac{1}{2}\theta_p$ and $\frac{1}{2}\theta_p$ around the stable zero torque position. For these angular shift values the axial force is positive and draws the two rotors together.

Figure 13 gives the evolutions of the stiffnesses (x,y and z) as a function of the angular shift between the rotors.
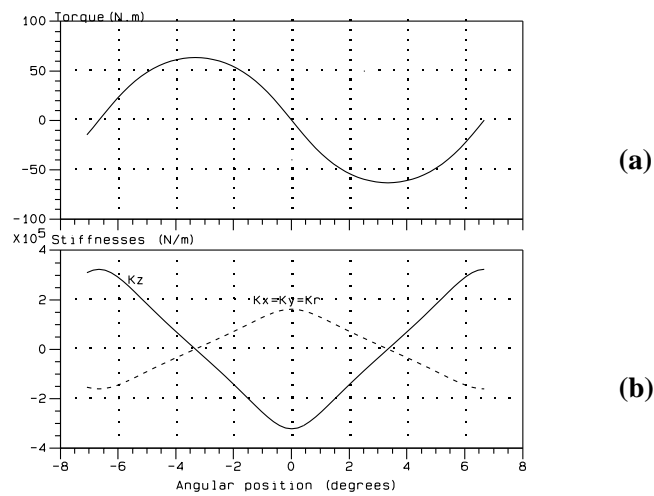

Figure 13: Torque (a) and stiffnesses (b)

We can notice that the stiffnesses in x and y directions are equal. The stiffness is the same for all elementary displacements in a plane perpendicular to the axis of the device. This common value can be called radial stiffness: K_r because it corresponds

23

to any displacement in a radial direction. We can verify that :

$$2.K_r(\theta) + K_z(\theta) = 0 \tag{13}$$

This relation is a direct consequence of the Earnshaw's principle (Earnshaw, 1839). We can see too that the maximal absolute values for the stiffnesses are obtained for the zero torque position. For the angular shift range which corresponds to the operating conditions ($\theta \in [-\frac{1}{2}\theta_p, \frac{1}{2}\theta_p]$), the radial stiffness is positive and the axial one is negative. That means that this device is stable for the displacements in the x,y plane. In this structure the magnetic forces contribute to maintain the rotors in a centered position (Yonnet,1981).

Zero stiffness Configuration

In this second part, we want to determine some particular configuration, for a plane air-gap coupling, which provides very interesting characteristics in terms of stability. The main dimensions of the coupling are the same than in the previous case : same number of pole pairs, same air-gap, same magnet and rotor thicknesses. In this study the core radius of the second rotor varies and the first rotor core radius remains constant and equal to 90 mm.

When the second rotor core radius varies the value of the stiffness which corresponds to the stable zero torque has been calculated. This value corresponds to the maximum absolute value of the stiffness when the angular shift between the rotors

24

varies. For all these configurations the pull-out torque and the maximal axial force have also been computed.

Figure 14 gives the evolution of the pull-out torque of the radial stiffness and the axial force as functions of the core radius of the second rotor.

We can notice that there are two configurations where the radial stiffness (and, as a consequence, the axial one) is nullified. These two configurations correspond to two values of the core radius of the second rotor, R_2 : $R_2 = 99.5mm$ and $R_2 = 80.3mm$.

In these configurations the radial and axial stiffnesses are nullified, but the axial force is not null. Nevertheless a solution exists to nullify this axial component of the force. A second magnet crown can be added symmetrically on one of the rotor as shown in Fig 15.

For symmetry reasons, in this new configuration the torque is doubled, the stiffnesses remain null and the axial force is nullified. That means that a small displacement in any direction of the leading rotor does not generate a force variation in the led rotor. The coupling run as a perfect mechanical filter and does not transmit vibrations. However the pull-out torque is lower than in the plane air gap classical structure (around 32 N.m for R2=99.5mm). This structure is quite similar to those found by Yonnet (Yonnet,1981) and Elies and al.(Elies,99)

25

Conclusion

In this paper we have proposed a method to calculate the mechanical behavior of PM couplings which is based on a semi-numerical integration of the forces between the magnets of the devices. This method is very efficient in terms of calculation time and precision and has been validated and compared with 3D FE in test cases. A general study of a plane air gap coupling with axially magnetized magnet has also been done using this semi-numerical method. This study shows that this method allows a systematic study of the magneto-mechanical characteristics of permanent magnet devices. This solution of calculation allows very good precision and small calculation time. So It can be used with success for the design of this kind of structure and the optimize them in terms of torque and stability.

References

Akoun G. and Yonnet J.P., (1984), "3D analytical calculation of the forces exerted between two cuboidal magnets", IEEE Transactions on Magnetics, Vol.20, No 5, pp. 1962–1964.

Bancel F. and Lemarquand G., (1998), "3D analytical optimization of Permanent Magnet alterned structure", IEEE Transactions on Magnetics, Vol.34, No 1, pp. 242–248.

Charpentier J.F. and Lemarquand G., (1999), "Optimal design of cylindrical air-gap synchronous Permanent Magnet couplings", IEEE Transactions on Magnetics, Vol.35, No 2, pp 1037–1046.

Elies P. and Lemarquand G., (1998), "Analytical optimization of the torque of a Permanent Magnet coaxial synchronous coupling", IEEE Transactions on Magnetics, Vol.34, No 4, pp 2267–2273.

Elies P. and Lemarquand G., (1999), "Analytical Study of radial stability of Permanent magnet synchronous couplings", IEEE Transactions on Magnetics, Vol.35, No 4, pp 2133–2136.

Earnshaw, (1839), "On the nature of the molecular forces which regulate the constitution of the luminiferous ether", Transactions Cambridge Philosophical society , Vol.7, Part 1, pp 97–112.

Feireira C. and Vaidya J., (1989), "Torque analysis of Permanent Couplings using 2D and 3D Finite Element Methods", IEEE Transactions on Magnetics, Vol.25, No 4, pp.3080–3082.

Furlani E.P., (1996), "Analysis and optimization of synchronous magnetic couplings", Journal of Applied Physics , Vol.79, No 8, pp 4692–4694.

-Furlani E.P., Wang R., and Kusnadi H., (1995), "A 3D Model for computing

the torque of radial couplings", IEEE Transactions on Magnetics , Vol.31, No 5, pp 2522–2526.

Giannini G.M., (1982), "Magnetic Couplings come of age", Mechanical Engineering, November issue, pp 54–56

Lemarquand V.,Charpentier J.F. and Lemarquand G., (1999), "Non sinusoidal torque Permanent Magnet couplings", IEEE Transactions on Magnetics, Vol.35, No 5, pp 4200-4205.

Overshott K.J., (1989), "The comparizon of the pull-out torque of Permanent Magnet couplings predicted theoretically with experimental measurements ", IEEE Transactions on Magnetics, Vol.25, No 5, pp 3913–3915.

Patterson T.N.L., (1968), "On Some Gauss and Labotto based integration Formulae", Math. Comp., Vol.22, pp.877–881.

Yonnet J.P., (1981), "Permanent Magnet bearings and couplings", IEEE Transactions on Magnetics, Vol.17, No 1, pp 1169–1173
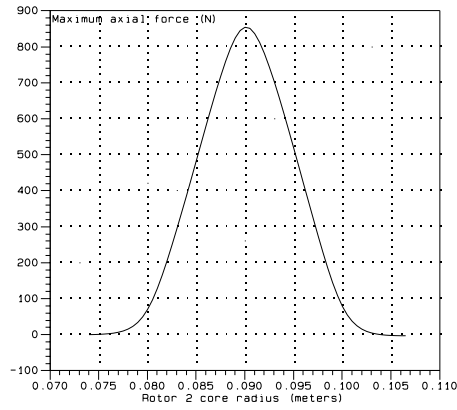
Wu W., Lovatt C., and Dunlop J.P., (1997), "Analysis and design of magnetic couplings using 3D Finite Element Modelling", IEEE Transactions on Magnetics, Vol.33, No 5, pp 4083–4085
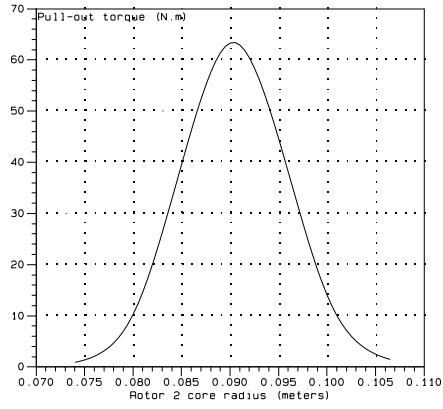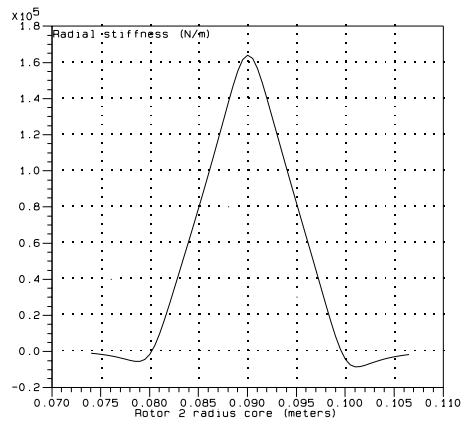
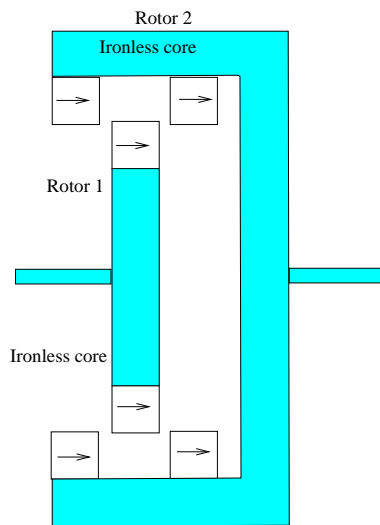Figure 14: Pull-out torque (a), radial stiffness (b) and maximum axial force (c)

Figure 15: Symmetrical structure